

On Controller Parametric Sensitivity of Passive Object Handling in Space by Robotic Servicers

Georgios Rekleitis, *Student Member, IEEE* and Evangelos Papadopoulos, *Senior Member, IEEE*

Abstract— A planning and control methodology for manipulating passive objects using orbital servicers in zero gravity has been developed by the authors. In this work, a parametric sensitivity analysis of the proposed model-based control for the motion of the passive object, in terms of parametric uncertainties, is presented. A linearization methodology is used to provide a scheme with which the controller robust behavior, in terms of parametric uncertainty, can be ascertained a-priori, without the need of running experiments. The system robust performance is illustrated in realistic 3D scenarios and verified via simulations.

Index Terms—Space robotics, free-flying cooperative robots, object manipulation on orbit, controller parameter sensitivity.

I. INTRODUCTION

The commercialization of space and the proliferation of activities in space require systems capable of fulfilling tasks such as construction, maintenance, astronaut assistance, docking and inspection, or even orbital debris handling and disposal, that fall under the theme of On-Orbit Servicing (OOS). Some of these tasks can be performed by astronaut Extra Vehicular Activities (EVA) which are not only dangerous, but also subject to limitations such as the force/torque an astronaut can apply, the motions that can be performed or even EVA temporal constraints. To relieve astronauts from EVA, enhance performance and extend the range of feasible tasks, robotic servicers will be required.

Robotic OOS has been discussed in the last twenty years and a number of architectures have been proposed [1]. Important robotic tasks, such as orbital-construction parts handling, handling of fuel-less satellites, or tumbling debris handling and deorbiting, require passive object handling capabilities, a procedure in which the first step is the passive object secure grasp. Studies in this field provided several theoretical approaches [2], [3] some of which resulted in experimental servicers [4], [5]. However, actual handling of a secured passive object has not been studied adequately and issues such as large object handling remain open.

Although several prototype robotic servicers have been proposed and studied, [2]-[6], only a few studies exist concerning the dynamics and control during the autonomous handling of a secured object. Dubowsky et al. proposed a control method aiming at reduction of flexibility-induced vibrations [7]. Nevertheless, in several cases, due to size and

low accelerations, the object flexibilities can be neglected, while both in orbital debris handling and construction, a wide variety of rigid bodies that must be handled, exists. Other methods were proposed to maintain firm grasp [8], or to secure contact with the environment [9]. Everist et al. proposed a free-flying servicer concept for handling and assembling space construction rods, using proportional thrusters under PD control [10]. Orbital system thrusters, though, are on-off devices, leading to limit cycles that reduce positioning accuracy and increase fuel consumption, compared to continuous control. To tackle this problem, Rekleitis and Papadopoulos proposed the use of a number of manipulator-equipped servicers, where both on-off thruster propulsion and manipulator continuous forces/ torques are used in object handling, [11], [12], see Fig. 1. It was shown that this approach leads to smaller tracking errors and less fuel consumption, while the object error tracking under a model based PD control was shown to be asymptotically stable [12]. However, the main drawback of this method is that, like all model-based controllers, it can be sensitive to parameter variation issues, a subject that remains open.

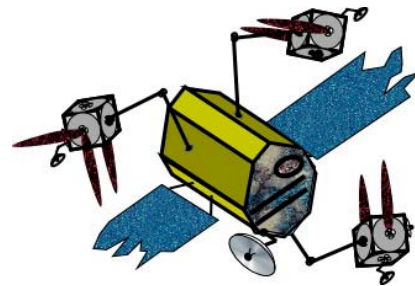


Figure 1. Concept of non-operational satellite handling, by a number of manipulator equipped cooperating free-flyers, in active debris removal task.

Parametric uncertainty can be treated with two main approaches; adaptation and robustness. In adaptive control, controller parameters are adapted so that the desired response is obtained despite parameter variations [13], [14], [15]. However, they are subject to limitations [16]. Robust methods ensure controller robustness, or bounded sensitivity to parametric uncertainty resulting in bounded errors, a priori known. The nonlinear robustness and parameter sensitivity field is rather limited, [17]. Most works focus on systems with special features, using them to prove stability under uncertainty (e.g. [18], [19]). Linearization can be employed so that linear system robustness and parametric sensitivity tools can be used, [20].

In this paper, we address the question of model-based PD control parametric uncertainty sensitivity and its effects on

Georgios Rekleitis and Evangelos Papadopoulos are with the Department of Mechanical Engineering, National Technical University of Athens, Greece (e-mail: [georek, egpapado]@central.ntua.gr; phone: +30-210-772-1440).

the response of the controller in [12], during passive object controlled motion, is studied via a linearization methodology. Assuming that parameters of the man-made servicers are adequately known, we focus on the passive object inertial properties (mass and inertia matrix), required for the chosen model-based PD control, [12]. Note that, even man-made passive objects can have uncertain inertial parameters, as in the case of satellite handling (active debris removal), damaged to unknown extent. It is shown that the passive object motion tracking errors vary within bounded values that can be obtained a-priori by knowing the desired trajectory and a bound in parameter uncertainty. This behavior is also demonstrated by simulations.

II. SPATIAL SYSTEM DYNAMICS AND CONTROL

Assume a passive object of mass m_0 and inertia matrix ${}^0\mathbf{I}_0$, where the subscript zero refers to the passive object. The zero superscript in ${}^0\mathbf{I}_0$ indicates that the inertia matrix is defined at the passive object body-fixed frame. A missing superscript indicates the inertial coordinate frame. On the object, a generalized force \mathbf{Q}_0 is applied by the end-effectors of a number of robotic servicers, see also [12]. Then, the equation of motion of the object, is

$$\mathbf{H}_0\ddot{\mathbf{q}}_0 + \mathbf{C}_0(\dot{\mathbf{q}}_0, \dot{\mathbf{q}}_0) = \mathbf{Q}_0 \quad (1)$$

where \mathbf{q}_0 are the passive object generalized coordinates

$$\mathbf{q}_0^T = [\mathbf{r}_0^T, \boldsymbol{\theta}_0^T]^T = [x_0, y_0, z_0, \theta_0, \varphi_0, \psi_0]^T \quad (2)$$

where, $[x_0 \ y_0 \ z_0]^T$ is the position vector \mathbf{r}_0 and $[\theta_0 \ \varphi_0 \ \psi_0]^T$ denote the Euler angles $\boldsymbol{\theta}_0$ of the passive object. \mathbf{H}_0 is the 6×6 mass matrix of the passive object, with

$$\mathbf{H}_0 = \begin{bmatrix} \text{diag}(m_0, m_0, m_0) & \mathbf{0}_{3 \times 3} \\ \mathbf{0}_{3 \times 3} & \mathbf{E}_0^T \mathbf{R}_0^T {}^0\mathbf{I}_0 \mathbf{R}_0 \mathbf{E}_0 \end{bmatrix} \quad (3)$$

where $\mathbf{I}_{3 \times 3}$ is the 3×3 identity matrix, \mathbf{R}_0 is the rotation matrix transforming vectors from the passive object frame to the inertial frame and \mathbf{E}_0 is a 3×3 matrix mapping the passive object Euler rates $\dot{\boldsymbol{\theta}}_0$ to its angular velocity $\boldsymbol{\omega}_0$:

$$\boldsymbol{\omega}_0 = \mathbf{E}_0 \dot{\boldsymbol{\theta}}_0 \quad (4)$$

\mathbf{C}_0 is a 6×1 vector containing the nonlinear velocity terms,

$$\mathbf{C}_0 = \left[\mathbf{0}_{1 \times 3}, \left(\mathbf{E}_0^T (\mathbf{R}_0^T {}^0\mathbf{I}_0 \mathbf{R}_0^T \dot{\mathbf{E}}_0 \dot{\boldsymbol{\theta}}_0 + \mathbf{E}_0 \dot{\boldsymbol{\theta}}_0 \times \mathbf{R}_0^T {}^0\mathbf{I}_0 \mathbf{R}_0^T \mathbf{E}_0 \dot{\boldsymbol{\theta}}_0) \right)^T \right]^T \quad (5)$$

The model based PD controller for the passive object is

$$\mathbf{Q}_0 = \mathbf{C}_0 + \mathbf{H}_0(\ddot{\mathbf{q}}_{0d} + \mathbf{K}_{p0}\mathbf{e}_0 + \mathbf{K}_{D0}\dot{\mathbf{e}}_0) \quad (6)$$

where $\mathbf{e}_0 = \mathbf{q}_{0d} - \mathbf{q}_0$ and \mathbf{q}_{0d} is the desired trajectory for the passive object, and \mathbf{K}_{p0} and \mathbf{K}_{D0} are control gains. Assuming perfect knowledge of the system parameters, use of the controller (6) leads to passive object asymptotically stable motion, as can be proven by Lyapunov stability theory [12].

III. PARAMETRIC SENSITIVITY ANALYSIS

Assume now that there is some uncertainty in the estimation of the passive object mass m_0 and inertia matrix ${}^0\mathbf{I}_0$ and that

the estimates of the uncertain quantities used in the controller (6) are denoted by \hat{m}_0 and ${}^0\hat{\mathbf{I}}_0$ respectively, where $(\hat{*})$ is the estimated value of $(*)$. The corresponding matrices \mathbf{C}_0 and \mathbf{H}_0 become $\hat{\mathbf{C}}_0$ and $\hat{\mathbf{H}}_0$ respectively. Thus, (6) becomes:

$$\mathbf{Q}_0 = \hat{\mathbf{C}}_0 + \hat{\mathbf{H}}_0(\ddot{\mathbf{q}}_{0d} + \mathbf{K}_{p0}\mathbf{e}_0 + \mathbf{K}_{D0}\dot{\mathbf{e}}_0) \quad (7)$$

Uncertain matrices $\hat{\mathbf{H}}_0$ and $\hat{\mathbf{C}}_0$ can also be written as:

$$\hat{\mathbf{H}}_0 = \mathbf{H}_0 + \delta\mathbf{H} \quad (8)$$

and

$$\hat{\mathbf{C}}_0 = \mathbf{C}_0 + \delta\mathbf{C} \quad (9)$$

Eqs. (1) and (7), provide the passive object equations of motion, in the case of uncertain parameter estimations:

$$\mathbf{H}_0\ddot{\mathbf{q}}_0 + \mathbf{C}_0 = \hat{\mathbf{C}}_0 + \hat{\mathbf{H}}_0(\ddot{\mathbf{q}}_{0d} + \mathbf{K}_{p0}\mathbf{e}_0 + \mathbf{K}_{D0}\dot{\mathbf{e}}_0) \quad (10)$$

or equally

$$\begin{aligned} \ddot{\mathbf{q}}_0 &= \mathbf{g}(\mathbf{q}_0, \dot{\mathbf{q}}_0) = \\ &= \mathbf{H}_0^{-1}(\hat{\mathbf{C}}_0 - \mathbf{C}_0) + \mathbf{H}_0^{-1}\hat{\mathbf{H}}_0(\ddot{\mathbf{q}}_{0d} + \mathbf{K}_{p0}\mathbf{e}_0 + \mathbf{K}_{D0}\dot{\mathbf{e}}_0) \end{aligned} \quad (11)$$

Since $\mathbf{e}_0 = \mathbf{q}_{0d} - \mathbf{q}_0$, we have

$$\begin{aligned} \mathbf{q}_0 &= \mathbf{q}_{0d} - \mathbf{e}_0 = \mathbf{q}_{0d} + \delta\mathbf{q}_0 \\ \dot{\mathbf{q}}_0 &= \dot{\mathbf{q}}_{0d} - \dot{\mathbf{e}}_0 = \dot{\mathbf{q}}_{0d} + \delta\dot{\mathbf{q}}_0 \\ \ddot{\mathbf{q}}_0 &= \ddot{\mathbf{q}}_{0d} - \ddot{\mathbf{e}}_0 = \ddot{\mathbf{q}}_{0d} + \delta\ddot{\mathbf{q}}_0 \end{aligned} \quad (12)$$

Using (12) on the left-hand side of (11) and linearizing the right-hand side of (11) at the desired point \mathbf{q}_{0d} , we have:

$$\begin{aligned} \ddot{\mathbf{q}}_{0d} + \delta\ddot{\mathbf{q}}_0 &= \\ &= \underbrace{\mathbf{H}_0^{-1}(\hat{\mathbf{C}}_0 - \mathbf{C}_0) + \mathbf{H}_0^{-1}\hat{\mathbf{H}}_0(\ddot{\mathbf{q}}_{0d} + \mathbf{K}_{p0}\mathbf{e}_0 + \mathbf{K}_{D0}\dot{\mathbf{e}}_0)}_{f(\mathbf{q}_0, \dot{\mathbf{q}}_0)} \bigg|_{\substack{\mathbf{q}_{0d} \\ \dot{\mathbf{q}}_{0d}}} + \\ &+ \frac{\partial f}{\partial \mathbf{q}_0} \bigg|_{\mathbf{q}_{0d}} \delta\mathbf{q}_0 + \frac{\partial f}{\partial \dot{\mathbf{q}}_0} \bigg|_{\dot{\mathbf{q}}_{0d}} \delta\dot{\mathbf{q}}_0 + HOT \end{aligned} \quad (13)$$

where *HOT* stands for *Higher Order Terms*. Using (8) and (9), we obtain

$$f(\mathbf{q}_{0d}, \dot{\mathbf{q}}_{0d}) = \mathbf{H}_0^{-1}\delta\mathbf{C} + \mathbf{H}_0^{-1}\delta\mathbf{H}\ddot{\mathbf{q}}_{0d} + \ddot{\mathbf{q}}_{0d} \quad (14)$$

Thus, (13) becomes

$$\begin{aligned} \delta\ddot{\mathbf{q}}_0 &= \left(\mathbf{H}_0^{-1}\delta\mathbf{C} + \mathbf{H}_0^{-1}\delta\mathbf{H}\ddot{\mathbf{q}}_{0d} \right) \bigg|_{\mathbf{q}_{0d}} + \\ &+ \frac{\partial f}{\partial \mathbf{q}_0} \bigg|_{\mathbf{q}_{0d}} \delta\mathbf{q}_0 + \frac{\partial f}{\partial \dot{\mathbf{q}}_0} \bigg|_{\dot{\mathbf{q}}_{0d}} \delta\dot{\mathbf{q}}_0 + HOT \end{aligned} \quad (15)$$

We define the following

$$\frac{\partial f}{\partial \dot{\mathbf{q}}_0} \bigg|_{\dot{\mathbf{q}}_{0d}} = \mathbf{F}_{dD}, \quad \frac{\partial f}{\partial \mathbf{q}_0} \bigg|_{\mathbf{q}_{0d}} = \mathbf{F}_{dP} \quad (16)$$

Assuming we are close enough to the desired trajectory, the *HOT* of (15) become insignificant. Thus, (15) becomes

$$\delta\ddot{\mathbf{q}}_0 - \mathbf{F}_{dD}\delta\dot{\mathbf{q}}_0 - \mathbf{F}_{dP}\delta\mathbf{q}_0 = \left(\mathbf{H}_0^{-1}\delta\mathbf{C} + \mathbf{H}_0^{-1}\delta\mathbf{H}\ddot{\mathbf{q}}_{0d} \right) \bigg|_{\mathbf{q}_{0d}} \quad (17)$$

The right-hand side of (17) depends on the desired trajectory and on the small uncertainty terms $\delta\mathbf{C}$ and $\delta\mathbf{H}$. Therefore, it is a small, bounded term that drives the second order system of the left-hand side, which is essentially a passive second-order system. Differentiating f , given in (13), according to (16), we have

$$\mathbf{F}_{dD} = -\mathbf{K}_{D0} + \underbrace{\left(-\mathbf{H}_0^{-1}\delta\mathbf{H}\mathbf{K}_{D0} + \delta\mathbf{T}_1\right)}_{\mathbf{E}_D} \Big|_{\mathbf{q}_{0d}} \quad (18)$$

$$\delta\mathbf{T}_1 = \mathbf{H}_0^{-1} \frac{\partial\delta\mathbf{C}}{\partial\dot{\mathbf{q}}_0}$$

Note that, for no uncertainty ($\delta\mathbf{H} = \delta\mathbf{C} = \mathbf{0}$), the right-hand side of (18) becomes equal to $-\mathbf{K}_{D0}$ and thus negative definite. For large enough gains \mathbf{K}_{D0} and small enough, but not negligible, uncertainty, the term $-\mathbf{H}_0^{-1}\delta\mathbf{H}\mathbf{K}_{D0}$ is dominated by the $-\mathbf{K}_{D0}$ term. This, in fact, is true for the whole \mathbf{E}_D term, since $\delta\mathbf{T}_1$ is a small term depending only on the desired trajectory and the uncertainty. Thus, in this uncertainty area, with large enough control gains, \mathbf{F}_{dD} is negative definite. The same method can be used in order to show that \mathbf{F}_{dP} is also negative definite, since the term \mathbf{F}_{dP} is

$$\mathbf{F}_{dP} = -\mathbf{K}_{P0} + \underbrace{\left(-\mathbf{H}_0^{-1}\delta\mathbf{H}\mathbf{K}_{P0} + \delta\mathbf{T}_2\right)}_{\mathbf{E}_P} \Big|_{\mathbf{q}_{0d}} \quad (19)$$

$$\delta\mathbf{T}_2 = \frac{\partial\mathbf{H}_0^{-1}}{\partial\mathbf{q}_0}\delta\mathbf{C} + \mathbf{H}_0^{-1}\frac{\partial\delta\mathbf{C}}{\partial\mathbf{q}_0} + \left(\frac{\partial\mathbf{H}_0^{-1}}{\partial\mathbf{q}_0}\delta\mathbf{H} + \mathbf{H}_0^{-1}\frac{\partial\delta\mathbf{H}}{\partial\mathbf{q}_0}\right)\dot{\mathbf{q}}_{0d}$$

The need for negative definite matrices \mathbf{F}_{dD} and \mathbf{F}_{dP} can be used as a design tool. For a class of desired trajectories and a bounded range of expected uncertainty, a range of matrices \mathbf{E}_D and \mathbf{E}_P can be found and thus the minimum required control gains \mathbf{K}_{D0} and \mathbf{K}_{P0} can be obtained.

With negative definite matrices \mathbf{F}_{dD} and \mathbf{F}_{dP} , the second order system of (17) is stable. If there was a steady-state, the first and second derivatives of $\delta\mathbf{q}_0$ would be zero. However, the small, bounded term on the right-hand side of (17), is not constant during the trajectory tracking motion. Nevertheless, the closed-loop frequency of the controller (and the resulting bandwidth) can be high enough by design, so that the fastest frequency of the desired motion is far lower than the closed-loop frequency. This is a realistic practice for controller design, especially for motions in space, in which the desired trajectories are quite slow by design. Thus, the second order system of (17) responds as if the right-hand side is a quasi-constant driving term, as will be seen in Section IV. Then, the acceleration and velocity errors ($\delta\ddot{\mathbf{q}}_0$ and $\delta\dot{\mathbf{q}}_0$) tend to zero and position/orientation errors tend to

$$\delta\mathbf{q}_0 \rightarrow -\mathbf{F}_{dP}^{-1}\left(\mathbf{H}_0^{-1}\delta\mathbf{C} + \mathbf{H}_0^{-1}\delta\mathbf{H}\dot{\mathbf{q}}_{0d}\right) \Big|_{\mathbf{q}_{0d}} \quad (20)$$

Note that the vector on which the position/ orientation error is attracted is a-priori known, since it depends on the desired trajectory and on the uncertainty, for which we can

estimate its expected maximum range. Thus, if the following hypotheses apply:

1. The initial errors as well as the known vector on which the position/ orientation error is attracted are close enough to zero, so that the linearization that led to (17) is still valid (both valid assumptions for a trajectory tracking problem such as the one at hand, especially when using standard parameter identification methods [21]-[22], to lower the parametric uncertainty),
2. The control gains \mathbf{K}_{P0} and \mathbf{K}_{D0} are high enough that the claim for negative definite \mathbf{F}_{dD} and \mathbf{F}_{dP} is still valid, as discussed in conjunction to (18) and (19),
3. The controller bandwidth is high compared to the bandwidth of the desired motions, so that a quasi-steady-state response can be obtained.

then the original non-linear system of (1), with a control generalized force as in (7), is stable with tracking error:

$$\begin{aligned} \begin{bmatrix} \mathbf{e}^T & \dot{\mathbf{e}}^T \end{bmatrix}^T &= -\begin{bmatrix} \delta\mathbf{q}_0^T & \delta\dot{\mathbf{q}}_0^T \end{bmatrix}^T \rightarrow \\ \rightarrow \begin{bmatrix} \mathbf{F}_{dP}^{-1}\left(\mathbf{H}_0^{-1}\delta\mathbf{C} + \mathbf{H}_0^{-1}\delta\mathbf{H}\dot{\mathbf{q}}_{0des}\right) \Big|_{\mathbf{q}_{0d}} & \mathbf{0} \end{bmatrix} &= \boldsymbol{\epsilon}_0 \end{aligned} \quad (21)$$

where $\delta\mathbf{q}_0$ is defined in (12). Moreover, the system is immune to small disturbances that do not increase the tracking errors to values that invalidate the above hypotheses. Summing up, if the tracking errors are small and the disturbances are not severe, then the passive object motion is stable, provided that the above hypotheses, whose validity can be determined a-priori, hold.

Note that during its motion, the passive object passes alternatively through steady-state phases and phases of transient response to disturbances. These disturbances are of two main types. The first type is due to possible discontinuities in the desired accelerations of the passive object, which result in tracking errors.

The second type is a result of the fact that in the analysis, we have assumed smooth application of the required \mathbf{Q}_0 as shown in (7). During the development of the controller (see [12]), we require that for safety reasons the thrusters facing the passive object are turned off and that any force required to push a servicer away from the passive object, will be provided by its manipulator as an additional force. Moreover, for this repulsive force to act without disturbing the passive object motion, it must be compensated by adequate additional manipulator forces provided by the other servicers. To reduce the computational requirements of the calculation of these additional manipulator forces during the simulations, we allowed the total additional force to the object to be non-zero (but very small). Thus, every time this repulsive force is needed, a small but predictable disturbance acts of the passive object motion. Nevertheless, if the motion is slow enough (a realistic assumption, especially in space), the controller can overcome these small disturbances, with the tracking errors returning again to the pre-estimated values of (21), as will also be shown in Section IV.

For a system without uncertainty, then (8) and (9) yield

$$\delta\mathbf{C}=\delta\mathbf{H}=\mathbf{0} \quad (22)$$

Thus, from (21), we obtain

$$\begin{bmatrix} \mathbf{e}^T & \dot{\mathbf{e}}^T \end{bmatrix}^T \rightarrow \mathbf{0}_{6 \times 1} \quad (23)$$

This response is the expected one, since the system without uncertainty is asymptotically stable, as has been shown in [12]. This can also be seen by assuming no uncertainty on the linearized system described by (16), in which case it leads to

$$\delta\ddot{\mathbf{q}}_0 + \mathbf{K}_{D0}\delta\dot{\mathbf{q}}_0 + \mathbf{K}_{P0}\delta\mathbf{q}_0 = -(\dot{\mathbf{e}} + \mathbf{K}_{D0}\dot{\mathbf{e}} + \mathbf{K}_{P0}\mathbf{e}) = \mathbf{0} \quad (24)$$

which is equal to the undriven error-dynamics of the passive object, under the model-based controller of (6), in the case of no uncertainty. The second order (24) can be shown easily to be asymptotically stable, by Lyapunov stability theory.

Using an analytical form for the passive object inertia matrix, the above analysis can be further developed. The general form of the inertia matrix ${}^0\mathbf{I}_0$ is given by (25):

$${}^0\mathbf{I}_0 = \begin{bmatrix} \int_V (y^2+z^2)\rho dV & \int_V xy\rho dV & \int_V xz\rho dV \\ \int_V xy\rho dV & \int_V (x^2+z^2)\rho dV & \int_V yz\rho dV \\ \int_V xz\rho dV & \int_V yz\rho dV & \int_V (x^2+y^2)\rho dV \end{bmatrix} \quad (25)$$

where V is the passive object volume and ρ is its density. Assuming that the uncertainty is in the measurement of V and ρ and the distribution of ρ , the estimated \hat{V} and $\hat{\rho}$ are:

$$\begin{aligned} \hat{V} &= V + \delta V \\ \hat{\rho} &= \rho + \delta\rho \end{aligned} \quad (26)$$

The uncertainties in (26) also affect the passive object center of mass position and its size estimates, due to the integrals in (25). By defining the top-left element of ${}^0\mathbf{I}_0$ as ${}^0I_{0,xx}$, then the estimated top-left element of ${}^0\hat{\mathbf{I}}_0$ is:

$${}^0\hat{I}_{0,xx} = \int_V (y^2+z^2)\hat{\rho} dV \quad (27)$$

Eq. (27) can be written as:

$$\begin{aligned} \int_V (y^2+z^2)\hat{\rho} dV &= \int_V (y^2+z^2)\rho dV + \int_V (y^2+z^2)\delta\rho dV + \\ &+ \int_{\delta V} (y^2+z^2)\rho dV + \int_{\delta V} (y^2+z^2)\delta\rho dV \end{aligned} \quad (28)$$

Note that all terms of (28) are elements of appropriate inertia matrices. The last term on the right-hand side of (28) is an integration over a very small volume δV , of a term that is proportional to the very small term $\delta\rho$. This means that the last integral term is negligible, compared to the other three terms. Then, (28) becomes:

$$\begin{aligned} \int_V (y^2+z^2)\hat{\rho} dV &= \int_V (y^2+z^2)\rho dV + \int_V (y^2+z^2)\delta\rho dV + \\ &+ \int_{\delta V} (y^2+z^2)\rho dV \end{aligned} \quad (29)$$

Thus, from (27) and (29), we obtain:

$$\begin{aligned} {}^0\hat{I}_{0,xx} &= \underbrace{\int_V (y^2+z^2)\rho dV}_{{}^0I_{0,xx}} + \\ &+ \underbrace{\int_V (y^2+z^2)\delta\rho dV + \int_{\delta V} (y^2+z^2)\rho dV}_{\delta I_{0,xx}} \end{aligned} \quad (30)$$

Using the same method, we also obtain the remaining estimated elements of ${}^0\hat{\mathbf{I}}_0$. Thus, the estimated ${}^0\hat{\mathbf{I}}_0$ becomes:

$${}^0\hat{\mathbf{I}}_0 = {}^0\mathbf{I}_0 + \delta\mathbf{I} \quad (31)$$

where the $\delta\mathbf{I}$ matrix also has inertia properties. Matrices $\delta\mathbf{H}$ and $\delta\mathbf{C}$ of (8) and (9), based on (3), (5) and (31), become

$$\delta\mathbf{H} = \begin{bmatrix} \text{diag}(\delta m_0, \delta m_0, \delta m_0) & \mathbf{0}_{3 \times 3} \\ \mathbf{0}_{3 \times 3} & \mathbf{E}_0^T \mathbf{R}_0 \delta \mathbf{I} \mathbf{R}_0^T \mathbf{E}_0 \end{bmatrix} \quad (32)$$

and

$$\delta\mathbf{C} = \begin{bmatrix} \mathbf{0}_{1 \times 3} & \left(\mathbf{E}_0^T (\mathbf{R}_0 \delta \mathbf{I} \mathbf{R}_0^T \dot{\mathbf{E}}_0 \dot{\boldsymbol{\theta}}_0 + \mathbf{E}_0 \dot{\boldsymbol{\theta}}_0 \times \mathbf{R}_0 \delta \mathbf{I} \mathbf{R}_0^T \mathbf{E}_0 \dot{\boldsymbol{\theta}}_0) \right)^T \end{bmatrix} \quad (33)$$

where δm_0 in (32), is given by

$$\delta m_0 = \rho \delta V + \delta\rho V \quad (34)$$

Thus, (32) and (33) can be used directly in (21), to obtain the steady state error.

IV. SIMULATIONS RESULTS

To demonstrate the results of the sensitivity analysis, we study the case of a passive object in the shape of a homogenous rectangular body, of dimensions $a \times b \times c = 2\text{m} \times 3\text{m} \times 2\text{m}$ and density $\rho = 15 \text{ kg/m}^3$, which corresponds to a passive object mass equal to 180 kg. The object is handled by three single-manipulator servicers, whose end-effectors are in point contact with the object. Each servicer base has thrusters capable of producing forces and moments, reaction wheels, and a single PUMA-type manipulator. The free-flying servicers have mass of 70 kg each, and their base is a cube of 0.7 m side. The three contact points lie on the object surfaces with normal vectors parallel to the \mathbf{x}_B , $-\mathbf{x}_B$ and \mathbf{y}_B unit vectors of the object body-fixed axes. The servicer thrusters develop per axis a force of 20 N, while their trigger threshold is set to $f_i = 10$ N. For attitude control, the servicers have additional pairs of thrusters that develop torque of 2 Nm per axis, and reaction wheels that can develop continuous torques up to $n_i = 1$ Nm per axis. The above system parameters, including the object/ servicer mass ratio, the servicer thruster, and the reaction wheel capabilities, were chosen taking into account realistic scenarios. The simulations are run on Matlab/ Simulink.

The motion of the passive object and the three servicers is simulated next. The passive object is commanded to follow a trapezoidal velocity trajectory in all DOFs, see Table I. The accelerations were chosen to be compatible with the servicers force/ moment capabilities. There is an initial position error for the passive object, equal to $\mathbf{e}_{0_init} = 0.05 * [-1 \ 1 \ 1] \text{m}$.

The control gains are constrained by reaction wheel and thruster limits. Higher gains would result in lower tracking errors, but also in more frequent thruster firing, resulting in higher fuel consumption. Given a desired motion, the tradeoff between tracking errors and fuel consumption can be used to obtain the appropriate gains. Here, the control gains in (7) are taken as $K_{p0} = 3.24$, $K_{D0} = 1.8$ (for all passive object *translational* DOF), $K_{p0} = 1.6$, $K_{D0} = 2.56$ (for all passive object *rotational* DOF). For more information on system parameters and control gains choice, refer to [12].

Table I. Passive object desired motion parameters (Trajectory 1).

DOF	const. accel. (m/s ²)/ (rad/s ²)	up to (s)	const. veloc. (m/s)/ (rad/s)	up to (s)	const. deccl. (m/s ²)/ (rad/s ²)	up to (s)
x_{0d}	0.0003	56	0.0168	84	-0.0003	140
y_{0d}	-0.00036	50	-0.018	90	0.00036	140
z_{0d}	0.0002	59	0.0118	81	-0.0002	140
θ_{0d}	$5 \cdot 10^{-5}$	60	0.003	80	$-5 \cdot 10^{-5}$	140
φ_{0d}	$7 \cdot 10^{-5}$	55	0.00385	85	$-7 \cdot 10^{-5}$	140
ψ_{0d}	10^{-4}	65	0.0065	75	-10^{-4}	140

Assuming uncertainty of +15%, -10% and +10% for the passive object dimension measurements, leads to an 11.4% volume uncertainty. This, in addition to a passive object density measurement uncertainty of -35.4%, results in an uncertainty regarding the passive object mass of about -20%. Thus, uncertainties $\delta\rho$ and δV in (26) are:

$$\delta\rho = 5.3 \frac{kg}{m^3}, \quad \delta V = 2.85 m^3 \quad (35)$$

Eq (35) is used in equations like (30) to provide the $\delta\mathbf{I}$ of (31), and in (34) to provide δm_0 . Then, $\delta\mathbf{I}$ and δm_0 are used in (32) and (33) to obtain $\delta\mathbf{H}$ and $\delta\mathbf{C}$, which in turn provide, through (21), the expected level of steady-state errors.

Fig. 2a shows the passive object tracking errors without uncertainty, i.e. with full knowledge of the parameters. As can be seen the controller overcomes the initial position errors within about 8 s, and position errors of that magnitude never reappear throughout the simulation. Fig. 2b is a zoom-in- e_0 -axis version of Fig 2a, showing more clearly the response after the controller reduces the initial position errors. This is to be contrasted with Fig. 2c, in which the uncertainty described above is taken into account. The controller reduces the initial position error and thus, in Fig. 2c we again focus in the zoom-in version of the response, for easier comparison with Fig 2b. The disturbance due to discontinuities in the desired accelerations of the passive object (see Table I), leads to the larger tracking errors during the transient phase, as can be seen in Figs. 2b and 2c and for the interval between 50s to about 90s. Also, the disturbances due to the application of the additional repulsive force are shown in Fig. 2b for the interval between 26s to 50s, 110s to 130s and 145s to 165s and in Fig. 2c for the interval between 26s to 50s, 100s to 115s and 125s to 135s. In both cases the controller rejects these disturbances as predicted, converging again to the expected error values, as can be seen both in Figs. 2 and 3. Even though the maximum tracking errors for

the system with uncertainty are larger than those for the system without uncertainty, they are still quite low.

Figures 3a and 3c show the upper six elements of the estimated steady-state errors vector $\boldsymbol{\varepsilon}_0$ (corresponding to \mathbf{q}_0), as obtained by (21). These are shown for two characteristic time spans during the simulation. Note that the lower six elements of $\boldsymbol{\varepsilon}_0$, corresponding to $\dot{\mathbf{q}}_0$, are constantly equal to zero throughout the simulation (not shown here for brevity).

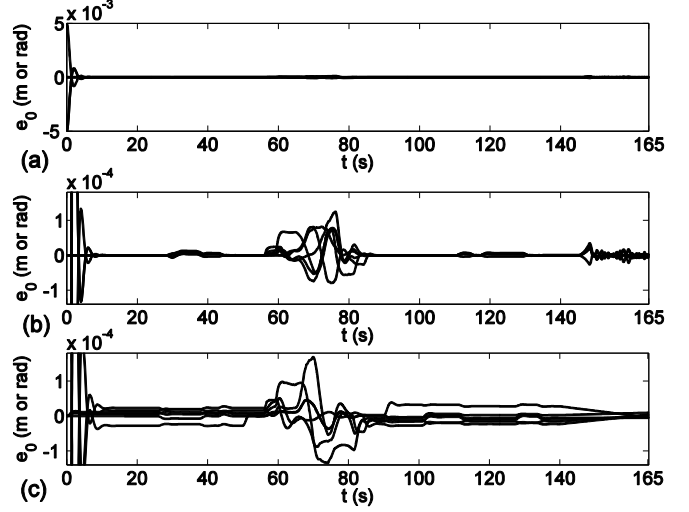


Figure 2. Tracking errors \mathbf{e}_0 for the passive object motion, for the system (a) and (b) without and (c) with uncertainty.

Throughout the simulation, the elements of $\boldsymbol{\varepsilon}_0$ are of the order of 10^{-4} or less (again not shown here for brevity) and thus this part of requirement (1) for (21) is verified. The actual position/orientation errors for the passive object, for the same time-spans, are shown in Fig. 3b and Fig. 3d respectively. The passive object tracking errors overcome the disturbances that have occurred and converge to the expected steady-state errors $\boldsymbol{\varepsilon}_0$.

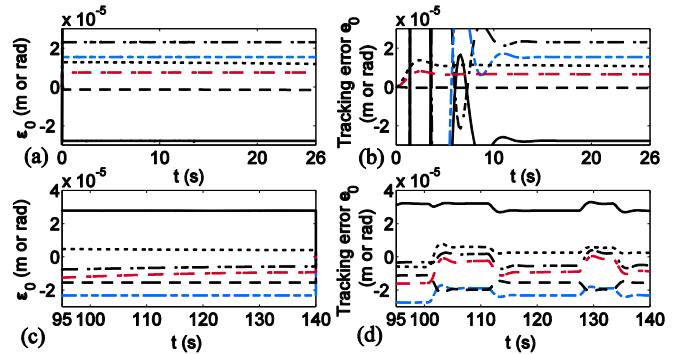


Figure 3. Comparison between expected position/orientation tracking errors (a and c) and the corresponding actual values (b and d), for two steady-state periods.

It should also be noted that as expected, all twelve elements of vector $\boldsymbol{\varepsilon}_0$ are constantly equal to zero throughout the simulation, in the case of no uncertainty ($\delta\rho = \delta V = 0$), verifying (22). This is not shown here for brevity.

In a simulation with a more demanding desired trajectory, a triangular profile on the desired velocities is used (no coasting), with higher accelerations, see Table II. The control gains and the uncertainty levels are as before.

Table II. Passive object desired motion parameters (Trajectory 2).

DOF	const. accel.	up to	const. deccel.	up to
x_{0d}	0.0004 (m/s ²)	70 (s)	-0.0004 (m/s ²)	140 (s)
y_{0d}	-0.00046 (m/s ²)	65 (s)	0.00046 (m/s ²)	130 (s)
z_{0d}	0.0003 (m/s ²)	75 (s)	-0.0003 (m/s ²)	150 (s)
θ_{0d}	$6 \cdot 10^{-5}$ (rad/s ²)	67 (s)	$-6 \cdot 10^{-5}$ (rad/s ²)	134 (s)
φ_{0d}	$7 \cdot 10^{-5}$ (rad/s ²)	73 (s)	$-7 \cdot 10^{-5}$ (rad/s ²)	146 (s)
ψ_{0d}	$1.1 \cdot 10^{-4}$ (rad/s ²)	70 (s)	$1.1 \cdot 10^{-4}$ (rad/s ²)	140 (s)

The tracking errors for this trajectory are shown in Fig. 4a for the case with uncertainty, again with zoom in e_0 axis for better comparison. A noticeable fact is that there are fewer disturbances, compared to the previous trajectory, since in this case there are fewer discontinuities in the desired trajectory (compare Fig. 4a to Fig. 2b, from about 50s to about 95s), although these are now somewhat larger, since the motion is faster and the discontinuities more abrupt. In the remaining of Fig. 4, the passive object tracking errors are compared to the expected values, for time periods where no disturbances occur. Again, the tracking errors converge on the corresponding steady-state values of ϵ_0 .

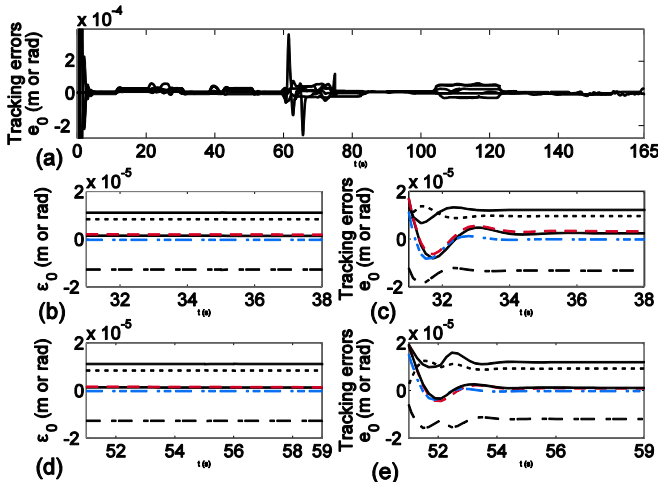


Figure 4. Passive object tracking errors e_0 (a), and comparison between the expected position/orientation tracking errors (b and d) and the corresponding actual values (c and e), for the system with uncertainty.

V. CONCLUSIONS

Previous work by the authors led to a planning and control methodology for manipulating passive objects using orbital servicers. This work demonstrates the robustness of the employed model based PD controller, under the presence of passive object parametric uncertainty. Assuming adequately known parameters of the man-made servicers, we focus on the passive object inertia parameters, needed for the chosen model based PD control. Linearization methodology is used in order to provide a scheme with which the proposed controller's robust behavior can be ascertained a-priori, without the need to run experiments, by simple knowledge of the desired trajectory and a maximum expectancy in parameter estimation uncertainty. The system robust performance is also illustrated in a realistic 3D scenario and verified via simulations, in which, not only the tracking

errors of the system converge to the expected values, but also the response overcomes certain disturbances, imposed on the controller.

REFERENCES

- [1] A. Tatsch, N. Fitz-Coy, and S. Gladun, "On-orbit Servicing: A Brief Survey," *Performance Metrics for Intelligent Systems Conf.*, Gaithersburg, MD, August 15 - 19, 2006.
- [2] I. Rekleitis, E. Martin, G. Rouleau, R. L'Archevêque, K. Parsa, and E. Dupuis, "Autonomous Capture of a Tumbling Satellite", *J. of Field Robotics*, Special Issue on Space Robotics, 2007, 24(4), pp. 275-296.
- [3] D. Reintsema, J. Thaeter, A. Rathke, W. Naumann, P. Rank, J. Sommer, "DEOS – The German Robotics Approach to Secure and De-Orbit Malfunctioned Satellites from Low Earth Orbits," *i-SAIRAS*, Sapporo, Japan, 29 August – 1 September, 2010.
- [4] K. Yoshida, "ETS-VII Flight Experiments For Space Robot Dynamics And Control," *Int. Symposium on Experimental Robotics*, Waikiki, Hawaii, USA, December 10-13, 2000.
- [5] <http://www.darpa.mil/orbitalexpress/>
- [6] K. Yoshida, H. Nakanishi, "The TAKO (Target Collaborativize) Flyer: a New Concept for Future Satellite Servicing," *i-SAIRAS*, Canadian Space Agency, Quebec, Canada, June 18-22, 2001.
- [7] S. Dubowsky, P. Boning, "The Coordinated Control of Space Robot Teams for the On-Orbit Construction of Large Flexible Space Structures," *ICRA '07, Special Workshop on Space Robotics*, Rome, Italy, April 10-14, 2007.
- [8] T. Hiramatsu, N. Fitz-Coy, "Game Theoretic Approach to Post-Docked Satellite Control," *20th Int. Symposium on Space Flight Dynamics*, Goddard Space Flight Center, USA, September 24, 2007.
- [9] S. A. A. Moosavian, R. Rastegarij and E. Papadopoulos, "Multiple Impedance Control for Space Free-Flying Robots," *AIAA Journal of Guidance, Control and Dynamics*, 2005, Vol. 28, No. 5, pp. 939-947.
- [10] J. Everist, K. Mogharei, H. Suri, N. Ranasinghe, B. Khostnevis, P. Will, and W. Shen, "A System for In-Space Assembly," *IROS '04*, Sendai, Japan, September 28 - October 02, 2004.
- [11] G. Rekleitis and E. Papadopoulos, "Towards Passive Object On-Orbit Manipulation by Cooperating Free-Flying Robots," *ICRA '10*, Anchorage, Alaska, USA, May 03-08, 2010.
- [12] G. Rekleitis and E. Papadopoulos, "On On-Orbit Passive Object Handling by Cooperating Space Robotic Servicers," *IROS '11*, San Francisco, California, USA, September 25-30, 2011.
- [13] J. E. Slotine, W. Li, "Applied Nonlinear Control" *Prentice Hall*, 1991.
- [14] S. Abiko, G. Hirzinger, "Adaptive control for a torque controlled free-floating space robot with kinematic and dynamic model uncertainty," *IROS '09*, St. Louis, MO, USA, October 10-15, 2009.
- [15] N.-H. Thai-Chau, I. Sharf, "Adaptive reactionless motion for space manipulator when capturing an unknown tumbling target," *ICRA '11*, Shanghai, China, 9-13 May, 2011.
- [16] V. Dobrokhodov, et al., "Experimental Validation of L1 Adaptive Control: The Rohrs Counterexample in Flight," *AIAA J. of Guidance, Control, and Dynamics*, v. 34, n. 5, 2011, pp. 1311-1328.
- [17] H. K. Khalil, *Nonlinear Systems*, Prentice Hall, 2002.
- [18] J. Becedas, V. Feliu, H. Sira-Ramirez, "Control of Flexible Manipulators affected by Non-Linear Friction Torque based on the Generalized Proportional Integral Concept," *IEEE Int. Symposium on Industrial Electronics (ISIE)*, Vigo, Spain, June 4-7, 2007.
- [19] P. Aghabalaie, M. Hosseinzadeh, H. A. Talebi, M. Shafiee, "Nonlinear robust control of a biped robot," *IEEE Int. Symposium on Industrial Electronics (ISIE)*, Bari, Italy, July 4-7, 2010.
- [20] J. C. Doyle, K. Zhou, *Essentials of Robust Control*, Prentice Hall, 1997.
- [21] C. H. An, C. G. Atkeson, J. M. Hollerbach, *Model-based control of a robot manipulator*, MIT Press, 1988.
- [22] T. Furukawa, T. Sugata, S. Yoshimura, M. Hoffman, "An automated system for simulation and parameter identification of inelastic constitutive models," *Computer Methods in Applied Mechanics and Engineering*, 2002, 191(21-22), pp. 2235-2260.